MIXED CONVECTION OVER A HORIZONTAL PLATE WITH VECTORED MASS TRANSFER IN A TRANSVERSE MAGNETIC FIELD

F. S. IBRAHIM and F. M. HADY

Department of Mathematics, Faculty of Science, Assiut University, Egypt

(Received 26 February, 1985)

Abstract. An exact similarity solution is presented for developing mixed convection flows of electrically conducting fluids over a semi-infinite horizontal plate with vectored mass transfer at the wall which are subjected to an applied transverse magnetic field. This solution is given for the case of a wall temperature that is inversely proportional to the square root of the distance from the leading edge. By application of appropriate coordinate transformations, the governing momentum and energy boundary-layer equations are expressed as a set of coupled ordinary differential equations that depend on a magnetic parameter, the buoyancy parameter, and the Prandtl number. The shear stress, the total heat transfer, and the displacement thickness are calculated for different values of both buoyancy and magnetic parameters.

1. Introduction

The field of magnetohydrodynamic (MHD) heat transfer can be divided arbitrarily into two sections: one contains problems in which the heating is an incidental by product of the electromagnetic fields (as in such MHD divices as generators, pumps, etc.), and the second consists of problems in which the primary use of electromagnetic fields to control the heat transfer (as in the natural convection flows and aerodynamic heating). This study is devoted to the second class of problems, viz., the influence of magnetic field on combined or 'mixed' natural and forced convection heat transfer to electrically conducting fluids.

Extensive studies have been made on the combined forced and free convection MHD flows as by Georgantopoulos *et al.* (1979), Raptis *et al.* (1981), Mazumder *et al.* (1976), Tan and Wang (1968). The flow of an incompressible viscous fluid past an impulsively started, infinite, horizontal plate, in its own plane, was first studied by Stokes (1851). Recently, Georgantopoulos *et al.* (1979) studied the hydromagnetic free convection effects on the Stokes problem for an infinite vertical plate. Raptis *et al.* (1981) studied the effect of suction/injection on the hydromagnetic free convection flow of a viscous, incompressible, and electrically conducting fluid, past an infinite accelerated non-conducting, vertical plate with variable suction and heat flux. Mazumder *et al.* (1976) studied the flow of an electrically conducting liquid past an infinite porous plate in the presence of a uniform transverse magnetic field and in a rotating frame of reference, and deduced the flow and heat-transfer characteristics of the Ekman layer over the plate. Tan and Wang (1968) studied the steady state heat-transfer phenomena in an aligned flow past a semi-infinite flat plate in which the velocity and magnetic field vectors far

Astrophysics and Space Science **114** (1985) 335–344. 0004–640X/85.15

from the plate are parallel. They used a viscous, electrically conducting, incompressible fluid, as the working medium.

Earlier investigations (Schneider, 1979; Dey, 1982; Afzal and Hussain, 1984) on the OHD (ordinary hydrodynamic) mixed convection flow over a horizontal plate were confined to the nonmagnetic case. Schneider (1979) studied the effect of buoyancy forces and has shown the existence of similarity provided the wall temperature is prescribed as the inverse square root of the distance from the leading edge. Likewise, the work of Dey (1982), dealing with an extension of Schneider (1979) to mass transfer. The solutions (see Schneider, 1979; Dey, 1982) cover a limited range of buoyancy to forced convection parameter that do not include the strongly buoyant flows in aiding situations and nearly separating flows in opposing situations. Afzal and Hussain (1984) developed the solutions of Schneider (1979) to include the entire domain, beginning form purely free convection dominated to separated flows.

The aim of this work is to extend the previous works of Schneider (1979) and Dey (1982) to the MHD mixed convection flows over a horizontal plate. An exact similarity solution is presented for the case of both a wall temperature and the magnetic strength which are inversely proportional to the square root of the distance from the leading edge. Numerical results are obtained for the shear stress, the total heat transfer and the displacement thickness with vectored suction and injection for different values of the magnetic and buoyancy parameters. The velocity and temperature profiles are graphically represented and the previous results are discussed in the last section.

2. Formulation of the Problem

Consider a horizontal flate plate aligned parallel to an uniform free stream with velocity u_∞, density ρ_∞, and temperature T_∞. The flow over the plate is considered to be plane, laminar, and steady. We use a Cartesian coordinate system x, y with the origin at the leading edge of the plate. The applied magnetic field is primarily in the y-direction and varies in strength as a function of x. No externally generated electrical field is imposed. Ohm's law is assumed and the magnetic Reynolds' number of the flow is taken to be small so that the flow induced distortion of the applied magnetic field can be neglected. Constant transport coefficients (including electrical conductivity) are assumed, the Boussinesq approximation is applied, and the boundary-layer approximation is assumed to hold. Under these conditions, the equations of continuity, momentum, and energy are

$$\frac{\partial u}{\partial x} + \frac{\partial v}{\partial y} = 0\,, \tag{1}$$

$$u\,\frac{\partial u}{\partial x} + v\,\frac{\partial u}{\partial y} = -\frac{1}{\rho}\,\frac{\partial p}{\partial x} + \nu\,\frac{\partial^2 u}{\partial y^2} - \frac{\sigma B^2}{\rho}\,u\,, \tag{2}$$

$$\frac{1}{\rho}\,\frac{\partial p}{\partial y} = g\beta(T - T_\infty)\,, \tag{3}$$

$$u \frac{\partial T}{\partial x} + v \frac{\partial T}{\partial y} = \alpha \frac{\partial^2 T}{\partial y^2} ; \tag{4}$$

u and v are the velocities in the horizontal and vertical directions. ρ, ν, β, α, and σ are the density, kinematic viscosity, the thermal expansion coefficient, thermal diffusivity, and the electrical conductivity of the fluid. T, p, and B are the temperature, pressure, and the applied magnetic field.

If we introduce the dimensionless variables in the form

$$X = x/L , \qquad Y = \sqrt{\mathrm{Re}}\, y/L , \qquad U = u/u_\infty ,$$
$$V = \sqrt{\mathrm{Re}}\, u/u_\infty , \qquad \theta = \frac{T - T_\infty}{T^*} , \qquad P = (P - P_\infty)/\rho_\infty u_\infty^2 , \tag{5}$$

where $\mathrm{Re} = u_\infty L/\nu$ is the Reynolds number and the pressure is referred to p_∞, T^* represents a characteristic temperature difference between plate and free stream.

The boundary conditions in dimensionless forms as in the nonmagnetic case (cf. Schneider, 1979), for which the similarity solution is possible, are

$$U = u_w , \qquad V = -2v_w X^{-1/2} , \qquad \Theta = X^{-1/2} \quad \text{on} \quad Y = 0 , \qquad X > 0 ;$$
$$U = 1 , \qquad \theta = P = 0 \quad \text{as} \quad Y \to \infty . \tag{6}$$

Also for the similarity solution to be possible we choose the strength of the magnetic field in the form

$$B = B_0 X^{-1/2} . \tag{7}$$

The solution of these coupled nonlinear equations is facilitated by introducing a number of transformations. Introduce a stream function ψ such that $U = \partial\psi/\partial Y$, $V = -\partial\psi/\partial X$. The following similarity transformation (originally used by Schneider (1979) in the non-magnetic case) reduces the problem to the solution of ordinary differential equations

$$\eta = YX^{-1/2} , \qquad \psi = X^{1/2} f(\eta) ; \qquad \theta = X^{-1/2} \phi(\eta) . \tag{8}$$

These relations transform (1) through (8) into the following set of coupled ordinary differential equations

$$2f''' + ff'' + K\eta\phi - Mnf' = 0 ; \tag{9}$$

$$\frac{2}{\mathrm{Pr}} \phi'' + f\phi' + f'\phi = 0 ; \tag{10}$$

with the boundary conditions

$$f(0) = f_w = \text{const. (given)} , \qquad f'(0) = f'_w = \text{const. (given)} , \qquad \phi(0) = 1 ,$$
$$f'(\infty) = \phi(\infty) = 0 ; \tag{11}$$

where primes denote differentiation with respect to the similar variable η, Pr stands for the Prandtl number, $\mathrm{Mn} = \sigma B_0^2 L/\rho u_\infty = H^2/\mathrm{Re}$ is a magnetic parameter, H is the Hartmann number, and K is related to the Archimedes number Ar according to

$$K = \mathrm{Ar}/\sqrt{\mathrm{Re}}\,, \qquad \mathrm{Ar} = gL\beta_\infty T^*/u_\infty^2\,. \tag{12}$$

In technological applications, the total heat transfer Q_w, the wall shear stress $f''(0)$ (in dimensionless form), and the displacement thickness δ^* are often of great interest. In order to circumvent the difficulties linked to the singularity at the leading edge the total heat transfer Q_w is determined with the help of the heat flux equation in the form

$$Q_w = \rho_\infty C_p \int_0^\infty [(T - T_\infty)]_{x=l}\,\mathrm{d}y\,. \tag{13}$$

where l is the length of the plate (not to be confused with the characteristic length L) and c_p is the specific heat capacity at constant pressure. Introducing the dimensionless variables of Equation (5) and applying the similarity transformation (8), we obtain

$$\mathrm{St}^* = \sqrt{\mathrm{Re}}\,\mathrm{St} = \int_0^\infty \phi f'\,\mathrm{d}\eta\,, \tag{14}$$

where the Stanton number is

$$\mathrm{St} = Q_w/\rho_\infty u_\infty C_p T^* L\,. \tag{15}$$

The displacement thickness δ^* can be calculated from the relations

$$\delta^* = \int_0^\infty \left(1 - \frac{u}{u_\infty}\right)\mathrm{d}y = \sqrt{\frac{\nu x}{u_\infty}} \int_0^\infty [1 - f'(\eta)]\,\mathrm{d}\eta$$

$$= \sqrt{\frac{\nu x}{u_\infty}} \lim_{\eta\to\infty} [\eta - f(\eta)]\,. \tag{16}$$

3. Numerical, Results, and Discussion

The system of ordinary differential equations (9) and (10) subject to the boundary conditions (11) has been solved numerically by means of the fourth-order Runge–Kutta method with a systematic estimates of $f''(0)$ and $\phi'(0)$ by the shooting technique. Numerical computations were carried out on a VME-2955 computer for $\mathrm{Pr} = 0.7$, $f_w' = f_w = 0;\ \pm 0.1;\ \pm 0.2$, $0 \le k \le 1$ and $0 \le \mathrm{Mn} \le 1$. It is interesting to note that the wall heat transfer mode ($\phi'(0) = -\mathrm{Pr}\, f_w/2$) depends on f_w, which causes the boundary-layer fluid either to received heat from the wall ($f_w > 0$) or to transfer heat to the wall ($f_w < 0$). Also, the numerical values of $\phi'(0)$ can be verified with the exact values and were found to be in good agreement.

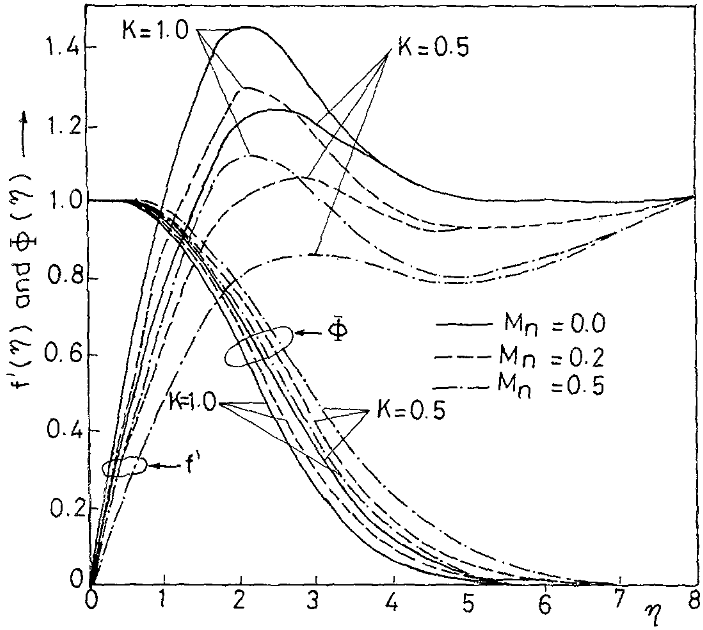

Fig. 1. Velocity and temperature profiles with no mass transfer ($f_w = f_w' = 0$) for various values of buoyancy parameter K and magnetic parameter Mn.

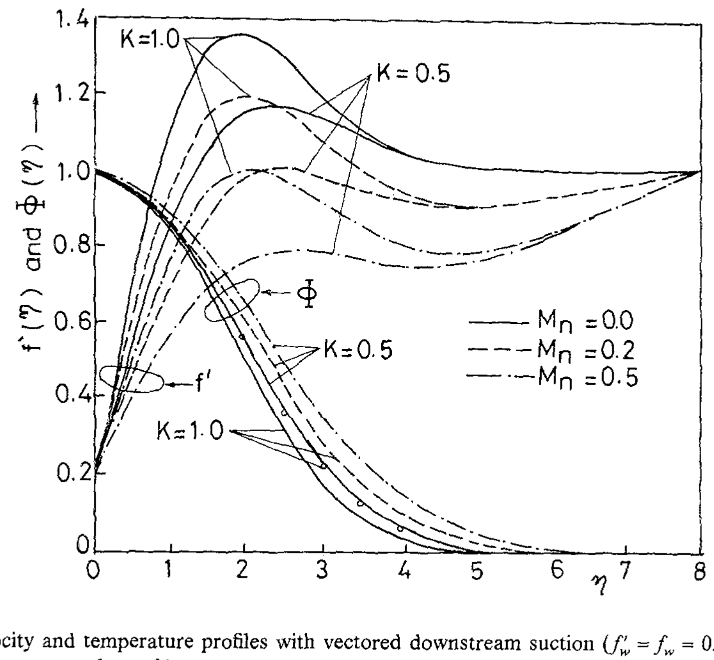

Fig. 2. Velocity and temperature profiles with vectored downstream suction ($f_w' = f_w = 0.2$) for various values of buoyancy parameter K and magnetic parameter Mn.

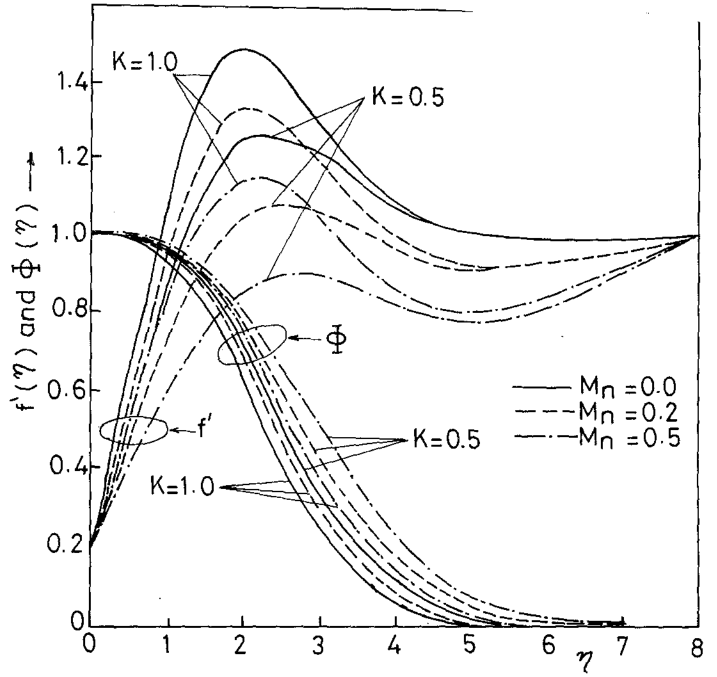

Fig. 3. Velocity and temperature profiles with vectored downstream injection ($f'_w = 0.2$, $f_w = -0.2$) for various values of buoyancy parameter K and magnetic parameter Mn.

Figures 1–3 illustrate the velocity and temperature profiles for different values of f'_w, f_w, k, and Mn, without mass transfer ($f'_w = f_w = 0$), with downstream vectored suction ($f'_w = f_w = 0.2$) and with downstream vectored injection ($f'_w = 0.2, f_w = -0.2$), respectively. It can be seen from Figures 1–3 that the velocity profile f' increases as the magnetic parameter Mn increases and it decreases as the buoyancy parameter increases. In the adverse case for the temperature profile ϕ. It is interesting to note that for large values of K and small values of Mn there are obviously overshoots in the velocity profiles, i.e., the local velocities are larger than the free-stream velocity. From Figure 3, it can be seen that both cases of ($K = 1.0$, Mn $= 0.2$) and ($K = 0.5$, Mn $= 0.0$) coincide. The same thing happens for the two cases ($K = 1.0$, Mn $= 0.5$) and ($K = 0.5$, Mn $= 0.2$).

Numerical results for the wall shear stress values $f''(0)$, the Stanton number St and the displacement thickness δ^*, which are not represented in Figures 4–6, are presented in Table I.

Figure 4 shows $f''(0)$, which is proportional to the wall shear stress, as a function of the buoyancy parameter K for different values of f'_w, f_w, and Mn. Figure 4 and Table I show that the buoyancy force ($K > 0$) enhances the wall shear values ($f''(0)$) as in the case of mixed convection without mass transfer ($f'_w = f_w = 0$). This is a consequence of there being a favorable pressure gradient above the plate due to buoyancy effects and the wall shear stress is larger than in the non-buoyant case (Schneider, 1979). On the

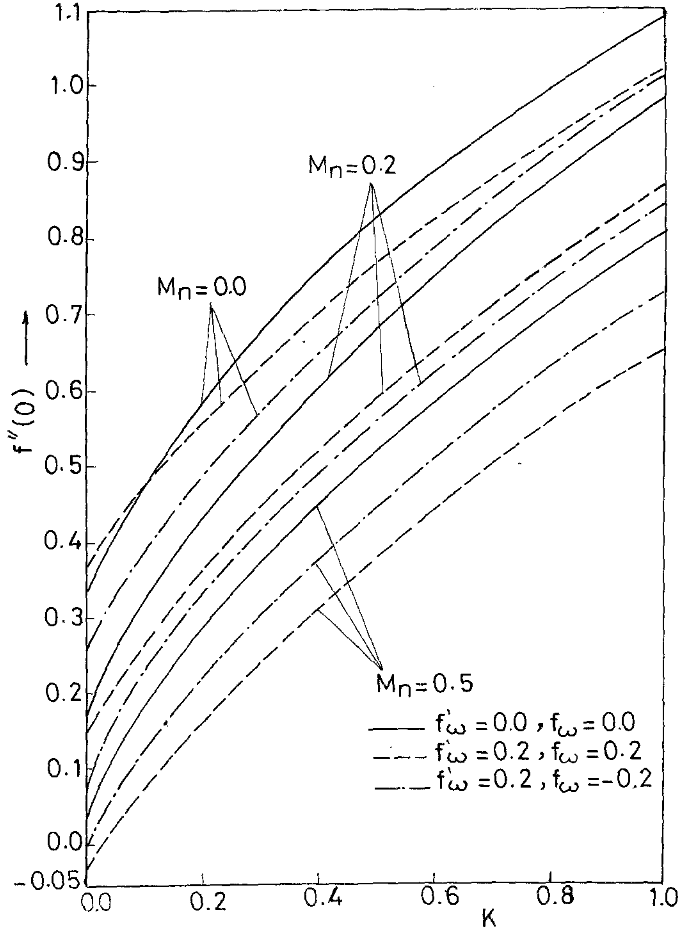

Fig. 4. Dimensionless wall shear values as a function of the buoyancy parameter K for various values of the magnetic parameter Mn and vectored mass transfer.

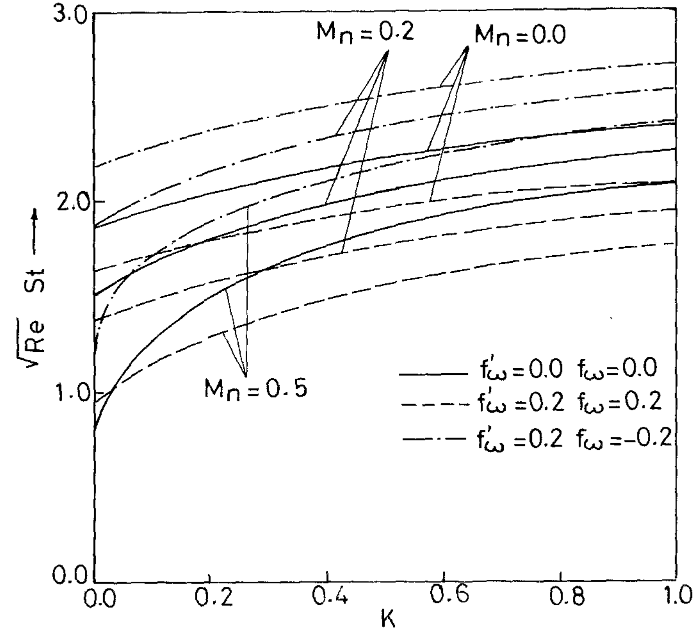

Fig. 5. Total heat transfer on the plante (Stanton number St) as a function of the buoyancy parameter K with vectored mass transfer for different values of the magnetic parameter Mn.

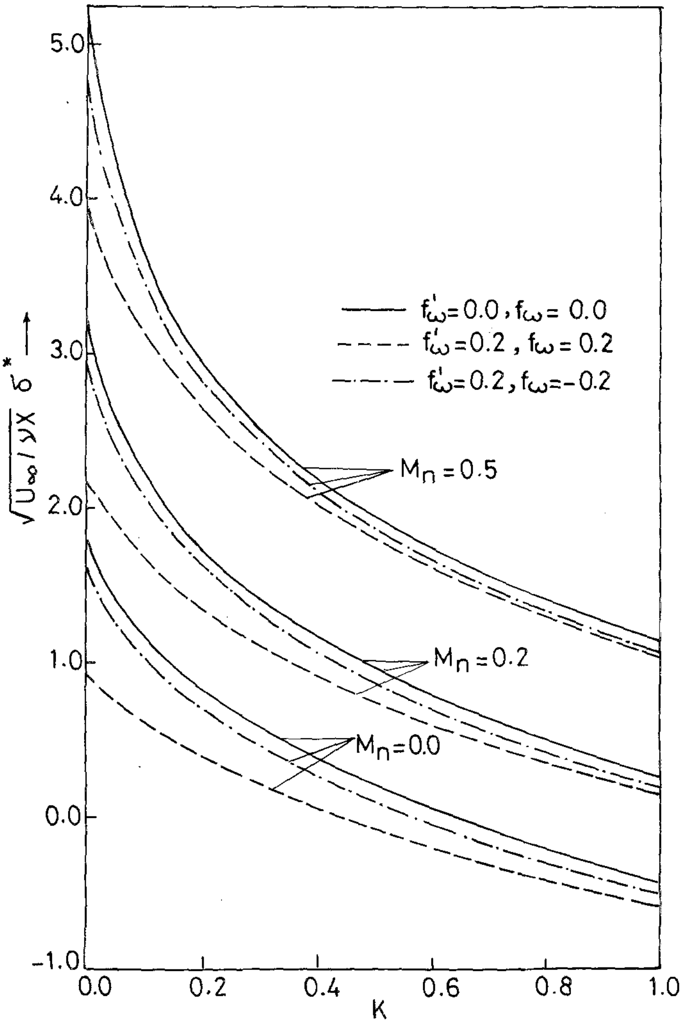

Fig. 6. Effect of buoyancy parameter K and magnetic parameter Mn on the displacement thickness δ^* with vector mass transfer.

other hand the magnetic force (Mn $>$ 0) reduces the wall shear values. It is showed that the wall shear values are higher with downstream-vectored suction ($f'_w = f_w = 0.2, 0.1$) than those with downstream-vectored injection ($f'_w = 0.2, 0.1$; $f_w = -0.2, -0.1$). It is interesting to note that for Mn $>$ 0 and $K > 0.15$ the wall shear values are higher with upstream-vectored injection ($f'_w = f_w = -0.1, -0.2$) than those with downstream-vectored suction ($f'_w = f_w = 0.1, 0.2$). Figure 4 and Table I show that, for Mn = 0.0 and $K < 0.15$, the wall shear values are higher with downstream-vectored suction than those with upstream-vectored injection which agree with Dey (1982) and Inger and Swean (1975).

TABLE I

Values of $f''(0)$, $\sqrt{\text{Re St}}$, and $\sqrt{u_\infty/\nu x}\,\delta^*$ for various values of f_w, f_w, K and Mn

Mn	K	$f'_w = -0.2, f_w = 0.2$			$f'_w = -0.2, f_w = -0.2$			$f'_w = 0.1, f_w = 0.1$			$f'_w = 0.1, f_w = -0.1$		
		$f''(0)$	$\sqrt{\text{Re St}}$	$\sqrt{u_\infty/\nu x}\,\delta^*$	$f''(0)$	$\sqrt{\text{Re St}}$	$\sqrt{u_\infty/\nu x}\,\delta^*$	$f''(0)$	$\sqrt{\text{Re St}}$	$\sqrt{u_\infty/\nu x}\,\delta^*$	$f''(0)$	$\sqrt{\text{Re St}}$	$\sqrt{u_\infty/\nu x}\,\delta^*$
0.0	0.0	0.403 860	1.533 516	1.931 613	0.203 548	2.276 968	3.313 636	0.359 009	1.730 155	1.271 186	0.295 946	2.009 979	1.628 746
	0.1	0.568 434	1.664 293	1.258 008	0.443 985	2.482 772	1.722 037	0.476 977	1.828 917	0.863 426	0.429 637	2.129 595	1.082 361
	0.2	0.687 053	1.746 067	0.877 813	0.586 339	2.542 822	1.171 328	0.573 362	1.901 010	0.580 792	0.533 406	2.209 682	0.740 253
	0.3	0.785 976	1.809 067	0.604 573	0.688 836	2.591 706	0.816 189	0.657 649	1.959 284	0.360 919	0.622 337	2.272 375	0.485 595
	0.4	0.783 130	1.861 411	0.388 841	0.782 425	2.634 214	0.550 235	0.733 863	2.008 834	0.179 563	0.701 884	2.324 804	0.208 816
	0.5	0.952 201	1.906 681	0.209 471	0.866 310	2.672 155	0.336 195	0.804 180	2.052 284	0.024 410	0.774 778	2.370 300	0.108 542
	1.0	1.278 226	2.075 552	−0.411 750	1.206 594	2.820 647	−0.371 787	1.101 645	2.217 219	−0.535 393	1.080 106	2.540 558	−0.497 227
0.2	0.0	0.223 245	1.152 036	3.643 798	0.089 036	0.807 284	5.776 979	0.164 895	1.443 437	2.632 302	0.120 852	1.686 069	3.090 895
	0.1	0.413 987	1.449 840	2.370 657	0.334 460	2.304 958	2.751 335	0.298 523	1.608 931	1.940 048	0.270 294	1.912 394	2.148 100
	0.2	0.536 749	1.563 237	1.835 653	0.467 885	2.400 887	2.036 523	0.400 045	1.707 884	1.538 287	0.377 504	2.022 878	1.672 252
	0.3	0.636 529	1.641 886	1.482 970	0.573 139	2.459 177	1.608 673	0.486 539	1.782 003	1.248 590	0.467 315	2.101 748	1.344 662
	0.4	0.723 507	1.704 363	1.216 568	0.663 820	2.506 758	1.298 936	0.563 743	1.842 504	1.019 808	0.546 836	2.164 864	1.092 136
	0.5	0.801 988	1.757 067	1.001 111	0.745 124	2.548 375	1.054 589	0.634 437	1.894 190	0.829 722	0.619 303	2.218 229	0.885 480
	1.0	1.123 673	1.947 111	0.284 645	1.075 661	2.708 699	0.270 780	0.930 626	2.082 960	0.173 491	0.920 963	2.410 862	0.187 408
0.5	0.0	0.139 469	0.430 354	5.424 205	0.095 395	0.224 004	6.739 623	0.006 548	0.937 206	4.488 212	−0.008 376	1.019 296	4.978 601
	0.1	0.292 373	1.115 872	3.770 638	0.250 225	1.897 226	4.028 332	0.132 735	1.292 779	3.360 066	0.124 378	1.580 129	3.526 218
	0.2	0.404 233	1.311 902	3.046 758	0.368 600	2.176 445	3.106 384	0.229 378	1.446 550	2.790 962	0.224 333	1.764 698	2.872 291
	0.3	0.496 148	1.420 656	2.602 450	0.463 345	2.273 657	2.599 463	0.311 522	1.547 019	2.410 172	0.308 355	1.873 626	2.454 494
	0.4	0.576 801	1.499 213	2.279 599	0.545 846	2.335 818	2.245 281	0.384 837	1.623 720	2.122 204	0.382 981	1.953 649	2.145 424
	0.5	0.649 952	1.562 408	2.024 717	0.620 434	2.385 019	1.971 206	0.452 631	1.686 786	1.889 627	0.451 192	2.018 311	1.898 991
1.0	0.0	0.154 088	0.091 935	6.419 514	0.130 020	0.052 187	7.150 473	−0.063 455	0.450 118	5.891 081	−0.062 097	0.482 746	6.229 893
	0.1	0.235 569	0.610 053	5.238 526	0.208 333	1.050 049	5.522 840	0.014 249	0.845 215	4.906 370	0.016 258	1.047 087	5.049 455
	0.2	0.316 292	0.929 485	4.444 566	0.296 085	1.705 803	4.408 148	0.087 629	1.083 264	4.252 441	0.092 266	1.370 728	4.286 495
	0.3	0.388 881	1.105 295	3.933 290	0.372 682	1.952 216	4.807 566	0.154 209	1.231 011	3.804 772	0.160 652	1.548 375	3.793 011
	0.4	0.454 825	1.218 810	3.567 525	0.440 921	2.072 264	3.408 251	0.215 390	1.338 215	3.470 705	0.223 068	1.664 213	3.436 524
	0.5	0.515 867	1.302 439	3.283 268	0.503 562	2.149 077	3.109 054	0.272 466	1.415 938	3.204 985	0.281 073	1.750 089	3.158 065
		0.777 033	1.558 902	2.394 159	0.769 657	2.364 664	2.201 229	0.519 472	1.675 028	2.349 024	0.531 022	2.014 250	2.278 995

Numerical results for the Stanton number St are shown in Figure 5. It is seen that as Mn increases the heat transfer rate decreases. On the other hand, as the buoyancy parameter increases the heat transfer rate increases. This happens because, for $K > 0$, the buoyancy accelerates the flow in the boundary layer.

The effect of the magnetic parameter Mn and the buoyancy parameter K on the displacement thickness δ^* with $f_w' = 0.2$ and $f_w = \pm 0.2$ is shown in Figure 6. It is interesting to note that the displacement thickness is negative for relatively large K, but it is positive for all nonzero magnetic parameter Mn. This is a consequence of local velocities that are larger than the mean velocity, cf. Figures 1–3.

References

Afzal, N. and Hussain, T.: 1984, *J. Heat Transfer* **106**, 240.
Dey, J.: 1982, *J. Heat Transfer* **104**, 558.
Georgantopoulos, G. A., Douskos, C. N., Kafousias, N. G., and Goudas, C. L.: 1979, *Letters in Heat and Mass Transfer* **6**, 397.
Inger, G. R. and Swean, T. F.: 1975, *AIAA J.* **13**, 616.
Mazumder, B. S., Gupta, A. S., and Datta, N.: 1976, *Int. J. Heat Mass Transfer* **19**, 923.
Raptis, A. A., Tzivanidis, G. J., and Perdikis, C. P.: 1981, *Letters in Heat and Mass Transfer* **8**, 137.
Schneider, W.: 1979, *Int. J. Heat Mass Transfer* **22**, 1401.
Stokes, G. G.: 1851, *Cambr. Phil. Trans.* **9**, 8.
Tan, C. W. and Wang, Carl C. T.: 1968, *Int. J. Heat Mass Transfer* **11**, 319.